



Electrochemical study of thiourea and substituted thiourea adsorbates on polycrystalline platinum electrodes in aqueous sulfuric acid

A.E. BOLZÁN*, R.C.V. PIATTI, R.C. SALVAREZZA and A.J. ARVIA

Instituto de Investigaciones Fisicoquímicas Teóricas y Aplicadas (INIFTA), (UNLP, CONICET), Sucursal 4, Casilla de Correo 16, (1900) La Plata, Argentina

(*author for correspondence, e-mail: aebolzan@inifta.unlp.edu.ar)

Received 30 October 2001; accepted in revised form 19 February 2002

Key words: adsorbates, adsorption isotherms, adsorption kinetics, dimethyl thiourea, methyl thiourea, platinum, tetramethyl thiourea, thiourea

Abstract

The electrochemical response of adsorbates produced on polycrystalline Pt from thiourea, methyl thiourea, 1,3 dimethyl thiourea and tetramethyl thiourea dissolved in aqueous 0.5 M sulfuric acid are comparatively studied using electrochemical routines. The adsorption kinetics of thioureas on Pt follows an Elovich-type equation. Their saturation coverage, measured from the decrease in the H-atom electroadsorption charge after correction for molecular size for steric effects, decreases as the size of the molecule producing adsorbates increases. Adsorption data fulfill the empirical Frumkin isotherm with a repulsive adsorbate–adsorbate lateral interaction term. Adsorbate electrooxidation starts at about 0.65 V vs SHE. The deprotonation of hydrogen-containing thioureas yields soluble products, their electrochemical behaviour being to some extent similar to that of formamidine disulfide. For $E > 0.65$ V vs SHE, the oxidation of thioureas can be described as complex processes in which intermediates compete with oxide layer formation on platinum.

1. Introduction

Thiourea (TU) is used as additive for copper electrodeposition and as inhibitor for copper corrosion [1, 2]. Recently, substituted thioureas have also been considered as possible additives for copper electrodeposition [3, 4]. Thioureas also behave to some extent as corrosion inhibitors. In both cases, their efficiency depends on their critical concentration and their chemical and electrochemical stability, the solution composition and cell operation. Optimal conditions are established largely by empirical means [5]. In principle, the presence of additives tends to modify the kinetics and mechanisms of electrochemical processes, as compared to those operative in additive-free baths. Generally, the interaction of thiol group-containing organic molecules such as TU, substituted TUs and derivatives of TUs with metal surfaces implies a reductive electrodesorption and oxidative electroadsorption at low potentials, molecular electrooxidation of adsorbates and TUs in solution through complex redox processes at an intermediate potentials, and the rupture of the C=S bond with the formation of C and S-containing species at high positive potentials [6]. Accordingly, the balance between the strength of the metal–S–C bond and that of the electric field at the reaction interface would determine the degree of influence of the additive on the kinetics and mech-

anism of the global process. However, no satisfactory answer to this issue is still available, because in many cases the chemistry of additive-containing solutions in contact with metal surface is far from understood. This includes, for instance, the possible formation of surface TU-metal complexes that might promote the formation of complex ionic and neutral species in solution.

Recent advances in the performance of aqueous copper electrode reactions in the presence of TU [7, 8] have shown that these reactions are complicated by simultaneous heterogeneous and homogeneous chemical reactions including TU protonation, TU-copper surface interactions and redox reactions of both TU and its electrooxidation products yielding complex ion formation [7, 9–11]. Therefore, on attempting to establish a rational use of additives it is convenient to explore the kinetics of those electrochemical reactions on different substrates, and a first approach to discriminate those different processes is to investigate copper electrode reactions in additive-containing solutions on a non-dissolving electrocatalytic metal such as platinum.

The adsorption of TU has been studied by different experimental techniques on copper [12–16], mild steel [17], silver [18], iron [19] and gold [20] electrodes. There is general agreement that the TU molecule is adsorbed perpendicularly with the S atom in the coordinating position [17, 20, 21] due to a strong chemisorption

process [12, 17, 20]. On the other hand Langmuir [16] or Frumkin [17, 20, 22] isotherms have been proposed to fit the experimental data. In the case of Frumkin isotherms, depending on the metal electrode, attractive interactions [20] or strong lateral repulsions [17, 22] have been observed.

This work refers to the electrochemical behaviour of TU, methyl thiourea (MTU), 1,3 dimethyl thiourea (DMTU) and tetramethyl thiourea (TMTU) dissolved in aqueous 0.5 M sulfuric acid on polycrystalline platinum, at 298 K, covering the potential ranges of additive adsorption and adsorbate electrooxidation. These results are useful to determine the influence of the number of methyl groups in the thioureas (TUs) on their electrochemical behaviour on platinum electrodes in terms of their surface coverage efficiency.

2. Experimental details

A conventional three-electrode cell using a polycrystalline (pc) platinum wire (Johnson Matthey, spec pure) as working electrode was utilized. The surface area of the working electrode was 0.4 cm^2 , as determined from the voltammetric hydrogen adsorption charge [24]. The working electrode surface was first polished with a water suspension of alumina ($0.3 \mu\text{m}$ grit), and subsequently washed repeatedly with Milli-Q water.

Working solutions were either aqueous 0.5 M sulfuric acid (base solution) or additive-containing base solution. The additive concentration (c_i , $i = \text{TU, MTU, DMTU, TMTU}$) was in the range $0 \text{ mM} \leq c_i \leq 1 \text{ mM}$. Solutions were prepared from Milli-Q water, sulfuric acid (98% Merck, p.a.), TU, MTU, DMTU and TMTU (all Fluka, puriss. p.a.). Occasionally, formamidine disulphide dihydrochloride (FDS)(ICN, 97%), or sodium sulphide (Merck, p.a.) dissolved in the base solution were also employed. For each experiment only freshly prepared solutions kept under nitrogen (99.99%) saturation were used.

The electrochemical setup consisted of a conventional potentiostat with wave generator, coupled to a Houston Omnigraphic recorder. Potentials were measured against a saturated mercurous sulfate reference electrode (MSE) but they are quoted on the SHE scale in the text. All runs were made at 298 K.

3. Results

3.1. Formation of adsorbed species

Adsorbates from TUs were formed by immersing the platinum electrode in the additive-containing solution for $0 \leq t_{\text{ad}} \leq 1400 \text{ s}$ holding the potential in the range $0.05 \text{ V} \leq E_{\text{ad}} \leq 0.45 \text{ V}$. Then, after the electrode was rinsed with water, it was immersed at $E = 0.45 \text{ V}$ in the base solution and a voltammogram was immediately started at $v = 0.05 \text{ V s}^{-1}$, from 0.45 down to 0.05 V,

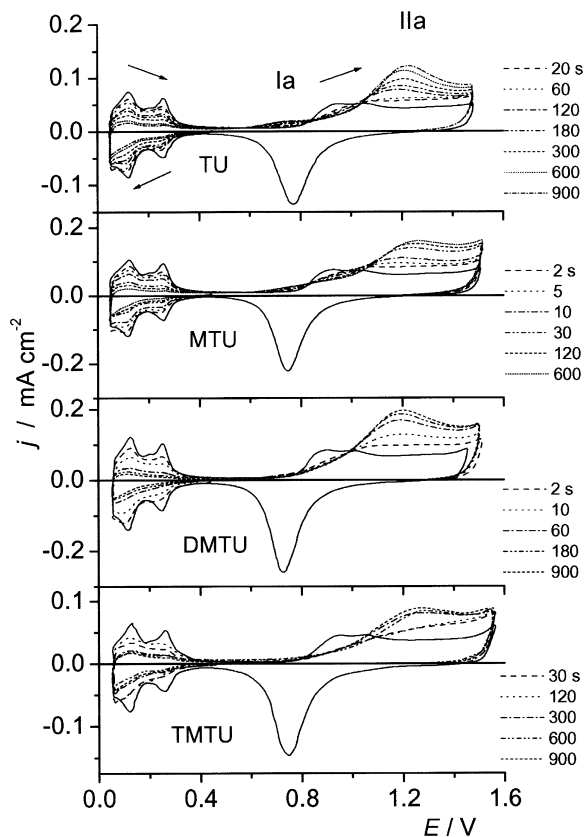


Fig. 1. First voltammogram run in 0.5 M H_2SO_4 from 0.45 to 0.05 V and from 0.05 to 1.5 V, for the electrooxidation of adsorbed species formed from TUs at $E_{\text{ad}} = 0.2 \text{ V}$ for different adsorption times. $c_i = 0.01 \text{ mM}$; $v = 0.05 \text{ V s}^{-1}$; 298 K.

then back to 1.5 V, and finally, down again to 0.05 V (Figure 1). For all TUs, as t_{ad} is increased the potential scan from 0.45 to 0.05 V shows a progressive decrease in hydrogen electroadsorption current. The following positive potential scan shows, from 0.4 to 1.4 V, the electrooxidation of adsorbates from TUs starting from 0.55 V upwards, and the appearance of peaks Ia and IIa at 0.75 V and about 1.25 V, respectively. The charge of these peaks increases with t_{ad} .

The presence of adsorbates also delays the formation of the oxygen-containing layer on platinum. The charge balance from the electrodesorption of adsorbates formed at $E_{\text{ad}} = 0.2 \text{ V}$ and $t_{\text{ad}} = 600 \text{ s}$ (Figure 1a) was determined after baseline correction. The charge of peak Ia, measured from 0.57 to 0.83 V, is $q_{\text{Ia}} \approx 0.04 \text{ mC cm}^{-2}$, and the charge of peak IIa evaluated from 0.83 to 1.5 V is $q_{\text{IIa}} \approx 0.42 \text{ mC cm}^{-2}$. This figure was obtained by subtracting the electroreduction charge of the oxygen-containing layer on platinum $q_{\text{ox}} \approx 0.261 \text{ mC cm}^{-2}$ resulting from 1.22 to 0.29 V, from the total electrooxidation charge $q_{\text{T}} \approx 0.68 \text{ mC cm}^{-2}$, determined from 0.83 to 1.5 V. For adsorbates from TU the peak IIa/peak Ia charge ratio from the first electrodesorption scan results in $q_{\text{IIa}}/q_{\text{Ia}} \approx 11$.

Similar experiments were run utilizing MTU, DMTU, and TMTU for $c_i = 0.01 \text{ mM}$ (Figures 1(b)–(d)). In general, these electrodesorption voltammograms resem-

ble to some extent those described for TU, except that the value of q_{Ia} decreases from TU to METU, and becomes practically nil for DMTU and TMTU (Figure 1(c)–(d)). In these three cases, peak IIa appears as a broad complex peak that shifts to lower potentials on going from MTU to DMTU (Figure 1(b)–(c)). Otherwise, the threshold potential for the electrooxidation of adsorbates from DMTU and TMTU is close to that for the initiation of the oxygen-containing layer on platinum [24]. From the voltammograms for MTU, DMTU and TMTU, for $t_{\text{ad}} = 10$ s and $E_{\text{ad}} = 0.4$ V, $q_{\text{IIa}} = 0.43 \pm 0.05$ mC cm⁻². This value was obtained by subtracting from $q_{\text{T}} \approx 0.80 \pm 0.05$ mC cm⁻² the total was electrooxidation charge from 0.83 to 1.5 V, $q_{\text{ox}} = 0.39 \pm 0.05$ mC cm⁻², the oxygen-containing layer electroreduction charge from 1.22 to 0.29 V. It should be noted that at constant t_{ad} , for the different TUs, the values of q_{IIa} almost the same. For the different TUs the number of voltammetric cycles required for the complete removal of adsorbates produced at constant E_{ad} increases with t_{ad} in the order TMTU > DMTU > MTU > TU.

In the potential range corresponding to the electroreduction of hydrogen on platinum, from 0.4 to 0.05 V, the anodic to cathodic charge ratio at $v = 0.05$ V s⁻¹ is always $q_{\text{a}}/q_{\text{c}} \approx 1$. Alternatively, the anodic charge ratio derived from the second and the first desorption scan are 1.79, 1.89, 2.15 and 2.35 for TU, MTU, DMTU and TMTU, respectively. This means that the inhibition capability for hydrogen atom electroreduction by adsorbates from TUs depends on the molecular size of TUs. This effect correlates with the projected area of adsorbates on platinum, as discussed further on. However, for $0.05 \leq E_{\text{ad}} \leq 0.5$ V the evolution of the voltammetric multiplicity of the hydrogen atom electroreduction peak remains practically the same, irrespective of t_{ad} and E_{ad} , as it would be expected for polycrystalline platinum surface sites that remains unaltered by the adsorption process.

3.2. Adsorbates from FDS-containing 0.5 M sulfuric acid

As FDS is the first main electrooxidation product from TU with an –S–S–bond, it was interesting to compare electrooxidation scans of adsorbates from FDS produced on platinum by immersion in 0.01 mM FDS + 0.5 M sulfuric acid (Figure 2) for different t_{ad} . These voltammograms show peaks Ia and IIa and the progressive decrease in hydrogen-atom electroreduction charge as t_{ad} is increased up to 600 s (Figure 2). The initial electroreduction scan produces new adsorbates from FDS that appear to be as those initially formed from TU (compare peaks Ia in Figures 1(a) and 2), although the rate of hydrogen atom electroreduction inhibition by adsorbates from FDS is about one order of magnitude higher than that observed for adsorbates from TU. Otherwise, for $t_{\text{ad}} > 100$ s peak Ia tends to disappear and peak IIa increases and shifts positively. These results suggest that for $4 \text{ s} \leq t_{\text{ad}} \leq 60 \text{ s}$, the adsorption of TU and FDS on platinum for

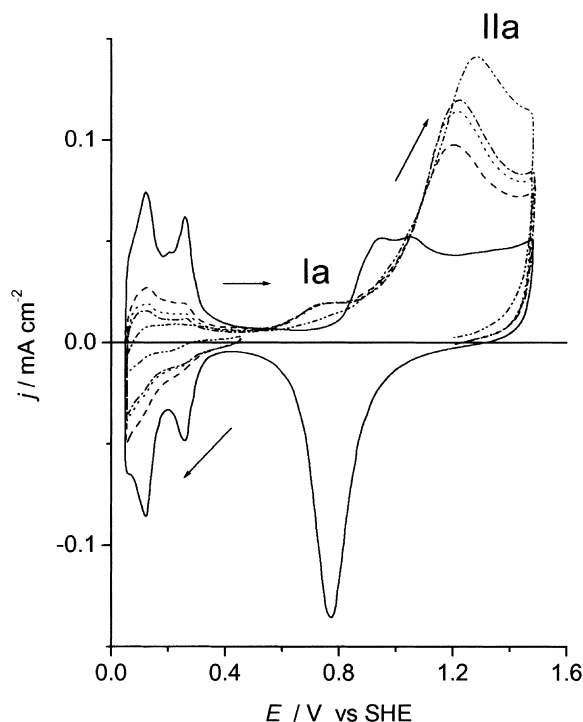


Fig. 2. Voltammograms in 0.5 M H₂SO₄ for the electrooxidation of adsorbed species formed from 0.01 mM FDS + 0.5 M H₂SO₄ at $E_{\text{ad}} = 0.2$ V for different t_{ad} . $v = 0.05$ V s⁻¹. 298 K. Key: (—) blank. t_{ad} : (---) 4, (·····) 10, (-·-·-) 20 and (-----) 600 s.

$0.05 \text{ V} \leq E_{\text{ad}} \leq 0.55 \text{ V}$ likely involves the formation of a common adsorbate. However, this adsorbate is not detected when $t_{\text{ad}} = 600$ s (Figure 2).

To compare the strength of chemical interactions between adsorbates produced by either TU or FDS on platinum, as well as their chemical stability, adsorbates were formed under open circuit by immersion in either 0.01 mM TU or 0.01 mM FDS + 0.5 M sulfuric acid for $t_{\text{ad}} = 300$ s. Subsequently, after water washing the electrode was transferred to the base solution to run a voltammogram from 0.45 to 0.05 V then to 1.5 V and backwards to 1.2 V at $v = 0.05$ V s⁻¹ (Figure 3). These voltammograms show that for the same t_{ad} either at open circuit or at constant potential, the surface coverage by adsorbates from FDS is larger than that by adsorbates from TU. Likewise, the voltammetric characteristics of adsorbed species are almost the same in spite of being produced either under open circuit or at E_{ad} in the range $0.05 \leq E_{\text{ad}} \leq 0.45$ V. However, the voltammetric charge related to adsorbates from FDS is greater than that of adsorbates from TU. Products formed in the potential range of peak IIa are electrochemically reduced in the range $0.05 \leq E \leq 0.5$ V.

3.3. Voltammetry from sodium sulfide-containing solutions

Voltammograms of platinum immersed in 1 mM sodium sulfide + base solution were run between 0.05 and 1.5 V as before at 0.05 V s⁻¹ for comparison with those

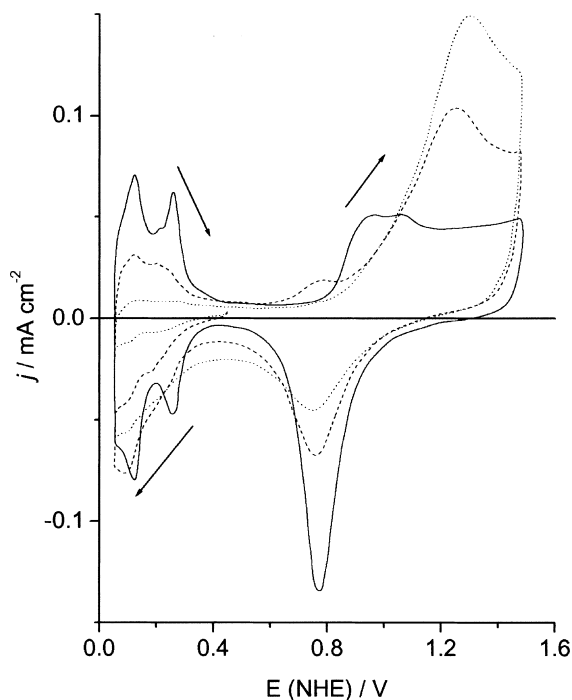
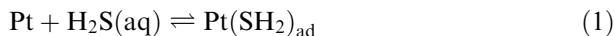
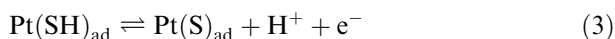
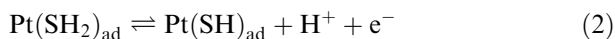


Fig. 3. Comparative voltammograms run in 0.5 M H₂SO₄ for the electrooxidation of adsorbed species formed under open circuit from 0.01 mM FDS + 0.5 M H₂SO₄ and 0.01 mM TU + 0.5 M H₂SO₄; $t_{ad} = 300$ s; $v = 0.05$ V s⁻¹; 298 K. Key: (—) blank. (---) 0.01 mM TU; (·····) 0.01 mM FDS.

resulting from solutions containing TU Figure 4(a). These experiments allowed us to find out the potential region where the electrooxidation of adsorbed sulfide takes place and identify products, such as sulfides, from the chemical or electrochemical decomposition of TU in acid [25, 26]. For $E < 0.15$ V, sulfide species strongly inhibit the electroadsorption of hydrogen atoms. This poisoning effect has been explained by the following reaction [27, 28]:



Conversely, at $E > 0.15$ V, other sulfur-containing adsorbates can be produced by electrooxidation reactions, such as



The presence of sulfur adsorbates also inhibits the hydrogen electroadsorption reactions [28].

Adsorbates from Reaction 3 and water are electrooxidized in the range $0.8 \leq E_{ad} \leq 1.3$ V yielding sulfate in solution [28, 29] and an oxygen-containing layer on platinum [24],

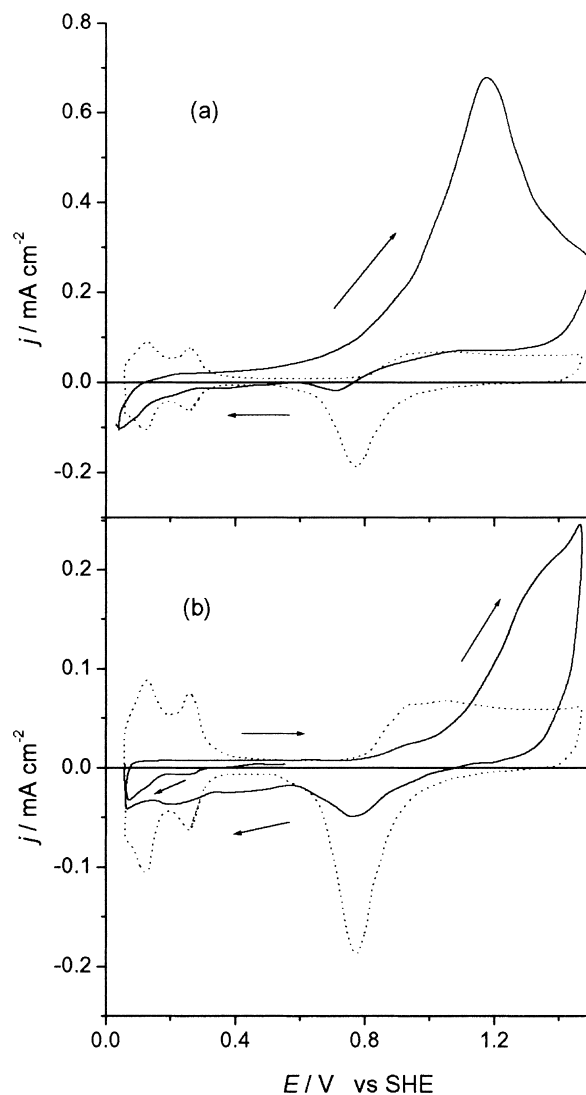
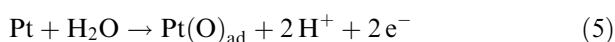


Fig. 4. Voltammogram of platinum run in (a) 1 mM Na₂S + 0.5 M H₂SO₄ and (b) in 0.5 M H₂SO₄ after immersion in aqueous 1 mM Na₂S for 30 s. Dotted lines correspond to the blanks; $v = 0.05$ V s⁻¹; 298 K.

The presence of sulfate ions during the electrooxidation of TU on platinum has been concluded from FTIR spectroscopy data [30, 31]. Reactions 4 and 5 account for the large anodic peak at about 1.25 V.

The voltammetric electrooxidation scan of platinum previously immersed in 1 mM sodium sulfide for $t_{ad} = 30$ s, (Figure 4(b)) shows that adsorbed sulfur also produces a strong inhibition of both hydrogen electroadsorption and the anodic peak at about 1.25 V. The anodic charge for Reaction 4 was estimated as $q_s = q_T - q_{ox}$. The total anodic charge measured from 0.7 to 1.55 V is $q_T = 1.24$ mC cm⁻², and the charge of oxide layer formation, measured from the oxide electroreduction peak, is $q_{ox} = 0.17$ mC cm⁻². Then, $q_s = 1.07$ mC cm⁻². The charge for the electrooxidation of a sulfur monolayer to sulfate ions is 1.26 mC cm⁻². Thus, the coverage of platinum by sulfur atoms is close to 80%. Similar charge balances resulted from the adsorption and electrooxidation of TU, MTU, DMTU and TMTU on platinum. Therefore, these adsorbates

behave in a similar way as far as their electrochemical reactivity is concerned.

3.4. Adsorption of carbon monoxide on platinum covered by adsorbates from TUs

The adsorption of CO on platinum electrodes covered by TU and TMTU was used as a test reaction to determine, for constant t_{ad} , the influence of the molecular cross section of TUs molecules on the maximum surface coverage by adsorbates, and correspondingly the adsorbate-free platinum surface area, provided that the adsorption is mainly non-dissociative and the amount of TUs-free platinum sites depends on the size of the TUs molecule.

For this purpose, adsorbates were produced by immersing the platinum electrode in aqueous either 0.01 mM TU or 0.01 mM TMTU + 0.5 M sulfuric acid for either 30 s or 900 s under open circuit. Subsequently, the electrode was washed with water and rapidly transferred to a glass tube under flowing carbon monoxide for 300 s, for the adsorption of carbon monoxide molecules on adsorbate-free platinum sites. Finally, the relative degree of surface coverage by carbon monoxide adsorbates (θ_{CO}) on TU and TMTU-adsorbates covered platinum was determined by voltammetry in aqueous 0.5 M sulfuric acid starting from 0.5 to 0.05 V, upwards to 1.4 V and finally back to 0.05 V at $v = 0.05 \text{ V s}^{-1}$ (Figure 5). This voltammogram shows a remarkable inhibition of hydrogen atom electroadsorption, in the range 0.5–0.05 V, a main anodic peak at about 0.9 V and two satellite current humps at about 0.8 V and 0.95 V, respectively. This complex peak, which is related to the electrooxidation of adsorbed carbon monoxide from platinum [32], suppresses the first electrooxidation peak (Ia) of TU and overlaps the electrooxidation current of TUs and the early stages of oxygen-containing layer formation.

For the case of TMTU charge balance one considers that the electrooxidation charge of $\text{CO}_{ad} + \text{TMTU}_{ad} + \text{Pt(O)}_{ad}$ is $q_T = 780 \mu\text{C cm}^{-2}$; the charge of oxide formation, estimated from the corresponding electroreduction charge, is $q_{r,ox} = 316 \mu\text{C cm}^{-2}$. Thus, the CO + TMTU electrooxidation charge results in $q_{\text{CO} + \text{TMTU}} = 464 \mu\text{C cm}^{-2}$. For the case of TU, the electrooxidation charge of $\text{CO}_{ad} + \text{TU}_{ad} + \text{Pt(O)}_{ad}$ is $q_T = 897 \mu\text{C cm}^{-2}$; the charge of oxide formation is $q_{r,ox} = 350 \mu\text{C cm}^{-2}$.

Finally, the carbon monoxide electrooxidation charge q_{CO} , estimated from the deconvolution of the carbon monoxide peak from the TMTU electrooxidation current contribution, is $q_{\text{CO}} = 240 \mu\text{C cm}^{-2}$, that is, about 52% of the CO + TMTU electrooxidation charge, and 60% of the theoretical electrooxidation charge for a full covered CO platinum surface [32]. For the case of TU-covered platinum electrode, the deconvoluted carbon monoxide electrooxidation charge is about $q_{\text{CO}} = 265 \mu\text{C cm}^{-2}$. Therefore, the electrooxidation charge of adsorbed TMTU results in $225 \mu\text{C cm}^{-2}$, whereas for

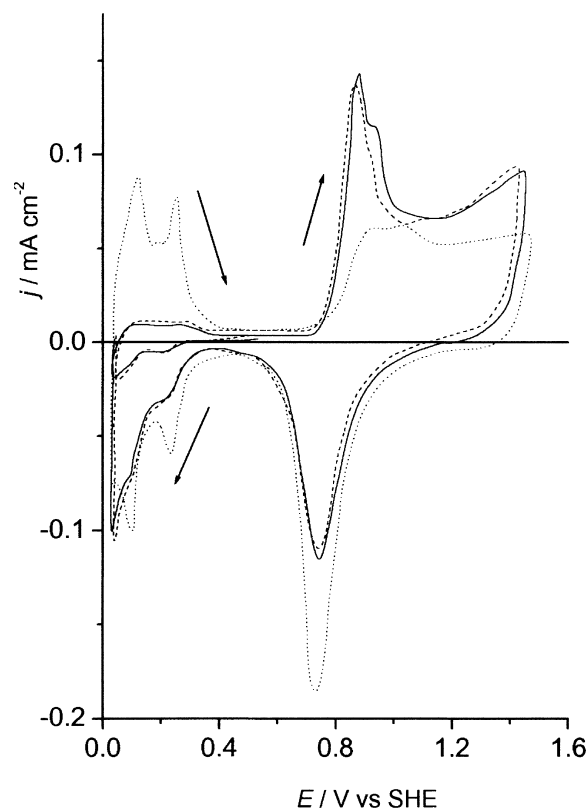


Fig. 5. Voltammetric electrooxidation of CO in 0.5 M H_2SO_4 adsorbed for 300 s on Pt. Previous to the CO adsorption the Pt electrode was immersed for 30 s in: 0.01 mM TU (dashed trace); 0.01 mM TMTU (full trace); $v = 0.05 \text{ V s}^{-1}$. Key: (—) CO + TU; (.....) CO + TMTU.

TU it is $285 \mu\text{C cm}^{-2}$. This means that under comparable conditions, the voltammetric charges for TU and TMTU adsorbate electrooxidation are about the same, that is, there is a compensation between the larger number of electrons per molecule required for the electrooxidation of TMTU, as compared to TU adsorbates, and the larger number of TU molecules that can be allocated on the platinum surface area. This is consistent with the charge balance observed for the electrooxidation of adsorbates from TU and TMTU at constant t_{ad} (Figure 1). The charge ratio for CO adsorbate electrooxidation in the presence of TMTU and TU results in about 0.9, that is, due to steric hindrance adsorbed TMTU leaves less free platinum sites for CO adsorption than TU adsorbates. These results are also consistent with the corresponding charge inhibition for the electroadsorption of hydrogen atoms.

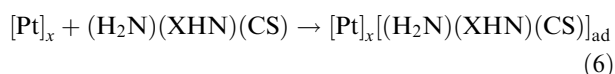
4. Discussion

4.1. Spontaneous and potential induced adsorbate formation from TU

The chemical or electrochemical formation of strongly bound adsorbates from TUs and FDS on platinum (Figures 1(a), 2 and 3) is consistent with the reactivity of

the CS bond of these molecules [33]. Data resulting from the application of different experimental techniques [6, 8, 10, 34–36] have shown that, under certain conditions, TU is adsorbed on copper [8, 10, 13, 16], gold [36], silver [35] and platinum [6] via the sulfur atom, i.e. by the formation of a thiol-type bonding. The initial formation of adsorbates from both TU and MTU at $E < 0.61$ V occurs without disruption of the molecule as recently reported for the case of TU adsorption on mono crystalline copper electrodes [16], albeit the stability of TU-adsorbates is still open to discussion [13, 36, 37].

Non-disruptive molecular interactions of TU and monosubstituted TUs with the platinum surface lead to molecular adsorbate formation,

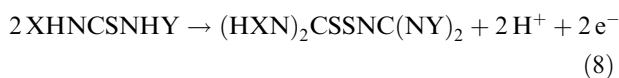


where $[\text{Pt}]_x$ denotes the number of platinum surface atoms involved in the adsorption of a single molecule of a TU and $\text{X} \equiv \text{H}$ or CH_3 group. Thus for TU, $x \approx 1$.

The oxidative electroadsorption and reductive electrodesorption of TU and partially substituted TUs involve a molecular deprotonation and a protonation reaction, respectively. For TU, the tautomeric form of the molecule presumably participates in these processes [38]:

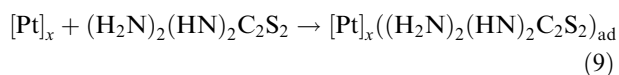


For TU and MTU peak Ia appears to be related to the formation of soluble disulfide species as the main product of the first electrooxidation stage. Accordingly, the similarities between the voltammograms for TU, MTU and FDS adsorbates, suggest that these reactions follow the general reaction path of thiols that are readily oxidized to disulfides, both as soluble and adsorbed species. The overall electrochemical reaction related mainly to peak Ia can be written as

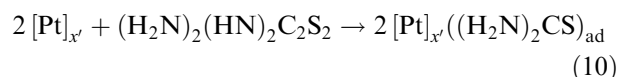


where $\text{X}, \text{Y} \equiv \text{H}$ or CH_3 group depending on the type of TUs considered. As concluded from the charge of peak Ia, the yield of Reaction 8 decreases in the order $\text{TU} > \text{MTU}$. This is consistent with the electrodecomposition of substituted TU yielding the type of species that are involved in the actual electrooxidation of TU. In all cases, soluble disulfide specie are probably produced via adsorbate formation on platinum, the surface concentration of these adsorbates decreasing on going from FDS or TU to MTU.

Similarly, FDS can also chemically interact with platinum, yielding either molecular disulfide adsorbate by a non-disruptive process



or by the rupture of the S–S bond



The formation of products other than dithio-compounds is also possible. As usually occurs in the electrooxidation of a number of organics [39], these reactions at $E > 1.0$ V involve the electrocombustion of adsorbates yielding soluble sulfate, carbon and nitrogen-containing products. The presence of these species in solution during the electrooxidation of TU and substituted TUs has been determined by FTIR spectroscopy [30, 31].

4.2. Surface coverage by adsorbates

As a first approximation, let us consider that the degree of surface coverage by hydrogen atoms can be used to determine the amount of adsorbates from TUs produced at constant potential and their evolution on potential cycling. Accordingly, the value of θ , the surface coverage by adsorbates, can be determined, in principle, from the ratio $\theta = q_h(0) - q_h(c)/q_h(0)$, where $q_h(0)$ and $q_h(c)$ refer to the hydrogen atom electroadsorption charge for $c_i = 0$ and $c_i = c$, respectively. Obviously, this approach overlooks the fact that the hydrogen atom and additive molecule cross sections are very different, so that a simple estimation of the coverage by additives from the decrease in hydrogen atom electroadsorption charge, would lead to an overestimation of the actual blockage by the different thioureas.

At constant c_i , E_{ad} and t_{ad} , the surface coverage by adsorbates from TUs depends considerably on the molecular structure of TUs. Thus, for $t_{\text{ad}} = 600$ s (Figure 6) strongly bound adsorbates from TUs block largely the platinum surface for hydrogen adatoms by about 70% for TU. This figure decreases as the size of the reacting molecule increases (Figure 6). The number of molecules required to attain full coverage is expected to decrease on going from TU to larger molecular size TUs. Correspondingly, under maximum monolayer coverage by adsorbates from TUs, the bare area left by these adsorbates should increase with their average cross section. In fact, as mentioned earlier, the cyclic electrodesorption voltammograms of TUs indicate that the hydrogen atom electroadsorption charge increases more rapidly as the average cross section of TU molecule increases, that is, the larger the molecule the greater the number of free sites left by its electrooxidation. Therefore, the values of θ obtained from the decrease in hydrogen electroadsorption charge should be corrected by the average molecular cross section of adsorbates from TUs.

Ab initio calculations showed that the group of atoms XHN– and X_2N – is almost free to rotate around the N–C bond axis with a solid angle that increases in size with the number and size of the substituent X in the group.

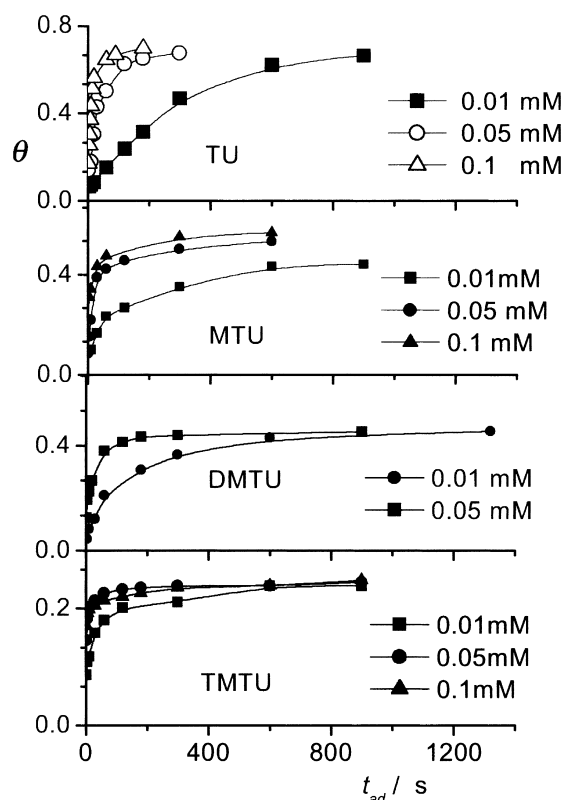


Fig. 6. θ_i against t_{ad} plots resulting from different concentrations of TU, MTU, DMTU and TMTU; $E_{ad} = 0.2$ V; 0.5 M H_2SO_4 ; 298 K.

This solid angle can be taken as a measure of the hindrance to the hydrogen adsorption reaction.

Considering that adsorbates from TUs are bound to the platinum surface via the sulfur atom [6], from the projected area of TU, MTU, DMTU and TMTU, the surface area blocked by each molecule of TUs was estimated as 8, 10, 12 and 19 \AA^2 , respectively. Thus, as the area of a single platinum site is about 6 \AA^2 , the screening of platinum surface sites by adsorbates increases by a factor ranging from about 1.3 to 3 platinum atoms on going from TU to TMTU. From the value of the area covered by the additive, the value of θ_i expected for each molecule (i) can be estimated from the ratio between the number of additive molecules and the number of platinum atoms per cm^2 (1.67×10^{15} atoms cm^{-2} for pc platinum). Then, it results in 0.75, 0.6, 0.5 and 0.3 for TU, MTU, DMTU and TMTU, respectively. It should be noted that these values are lower than those found from the experimental decrease in hydrogen atom adsorption charge (Figure 1), as expected. For substituted TUs, the value of θ_{max} is consistent with the closest approach distance of substituents (CH_3) in neighbour adsorbates. For TMTU it is 0.45 nm [40]. Furthermore, the steric hindrance for the adsorption of hydrogen atoms and carbon monoxide (Figure 5) should also be influenced by the specific geometry of the adsorbate standing either vertically or at least at an angle with respect to the surface electrode, as observed for TMTU adsorption on Au(1 1 1) [41]. It should be noted that despite the reasonable agreement between

experimental and calculated saturation coverages, experimental data represents the average behaviour of a polycrystalline surface, whereas estimations are based on a single crystal (1 1 1) face. For TU the estimated 0.75 value is in good agreement with that found for the adsorption of TU on Au(1 1 1) [36].

Alternatively, for non-disruptive adsorption, the increase in molecular size of TUs implies that a smaller number of these molecules is required to reach a maximum surface coverage of the substrate. Consequently, the electrochemical dimerisation to form the S-S bond should be gradually hindered as the size of the adsorbate is increased, in agreement with our experimental results.

The preceding corrections make it possible to approximate a definition of the true degree of surface coverage of platinum by adsorbates from TUs in terms of the same blockage of hydrogen atom electroadsorption. Thus, the number of TMTU molecules is half the number of TU molecules and the electrooxidation charge should be about twice the charge for TU, as found experimentally. This fact can also explain the small differences between the electrooxidation charges for MTU, DMTU and TMTU adsorbates, that is, the number of electrons per molecule increases from MTU to TMTU, and the number of molecules adsorbed on platinum decreases from MTU (~ 0.6 molecule) to TMTU (~ 0.3 molecule).

4.3. Adsorption kinetics

The kinetics of adsorption from TUs was followed through the decrease in the value of θ_H (Figure 6) and the increase in free surface sites from the first to the second electrodesorption cycles. The value of θ_H calculated from the decrease in the hydrogen atoms adsorption charge was corrected by the size of the adsorbing molecule, that is, the theoretical coverage by one additive molecule with respect to the platinum atom. Then, the true coverage can be expressed as $\theta_t = (q_h(0) - q_h(c)/q_h(0))\theta_m$, where $q_h(0)$ and $q_h(c)$ refer to the hydrogen atom electroadsorption charge for $c_i = 0$ and $c_i = c$, respectively, and θ_m is the area ratio between the additive molecule and the surface platinum atom site. For TU, MTU, DMTU and TMTU at constant c_i , the value of θ_t increases with t_{ad} , and the time required to attain adsorption saturation diminishes as c_i is increased (Figure 6). In all cases, for the time window of our experiments, a value of $q_h(c)$ is asymptotically attained with θ_t 's ranging from 0.75 for TU to 0.3 for TMTU. These figures would indicate that the rate of adsorption of thioureas on platinum increases in the order TU > DMTU > MTU > TMTU. Otherwise, no apparent influence of E_{ad} on the value of θ_t resulting from the adsorption of TU on platinum was observed (Sec. 3.1), as one would expect for the relatively strong Pt-TUs interactions.

The adsorption kinetics for the four thioureas fits a $\theta_t/\log t_{ad}$ linear relationship, although the range of θ_t

depends on the type of thiourea. This rate law can be described by the Elovich equation [42], that assumes that the activation energy E_a^* changes linearly with the surface coverage by the adsorbate according to $E_a^* = E_0^* + \alpha\theta_t$. Then, the adsorption rate equation becomes

$$\frac{d\theta_t}{dt} = Ac_i \exp\left[-\left(\frac{E_0^* + \alpha\theta_t}{RT}\right)\right] \quad (11)$$

where A is a preexponential factor, c_i is the concentration of the adsorbing species, and α is the variation of E_0^* with θ_t . After the integration of Equation (11)

$$\theta_t = B \log t_{ad} \quad (12)$$

This equation is reasonably fulfilled by the adsorption of TU, MTU, DMTU and TMTU (Figure 7).

4.4. Adsorption isotherms

The θ_t/t_{ad} plots show that saturation time depends on c_i and the type of TU considered, that is, as either c_i , or TU substitution is increased, saturation is attained

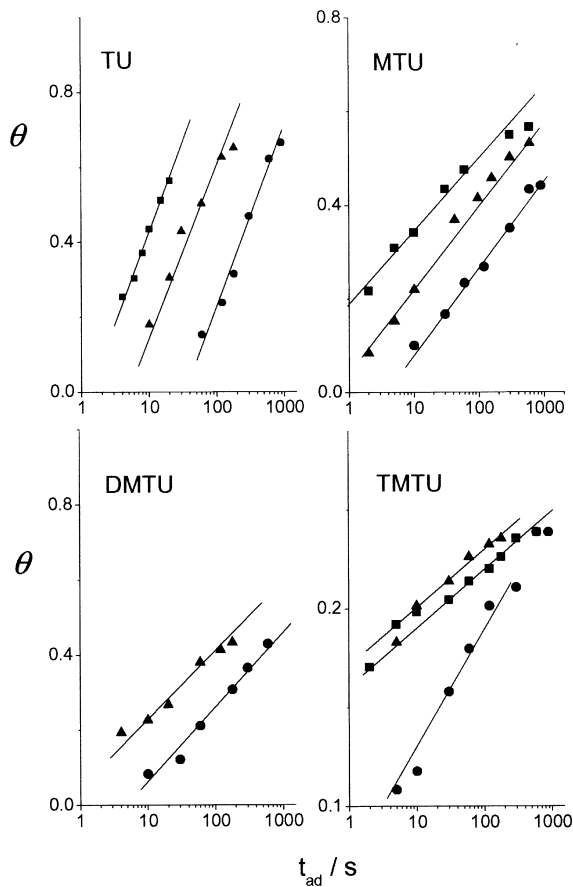


Fig. 7. θ_t against $\log t_{ad}$ plots for the adsorption of TU, MTU, DMTU and TMTU, for different concentrations: (■) 0.1 mM; (▲) 0.05 mM; (●) 0.01 mM; $E_{ad} = 0.2$ V; 0.5 M H_2SO_4 ; 298 K.

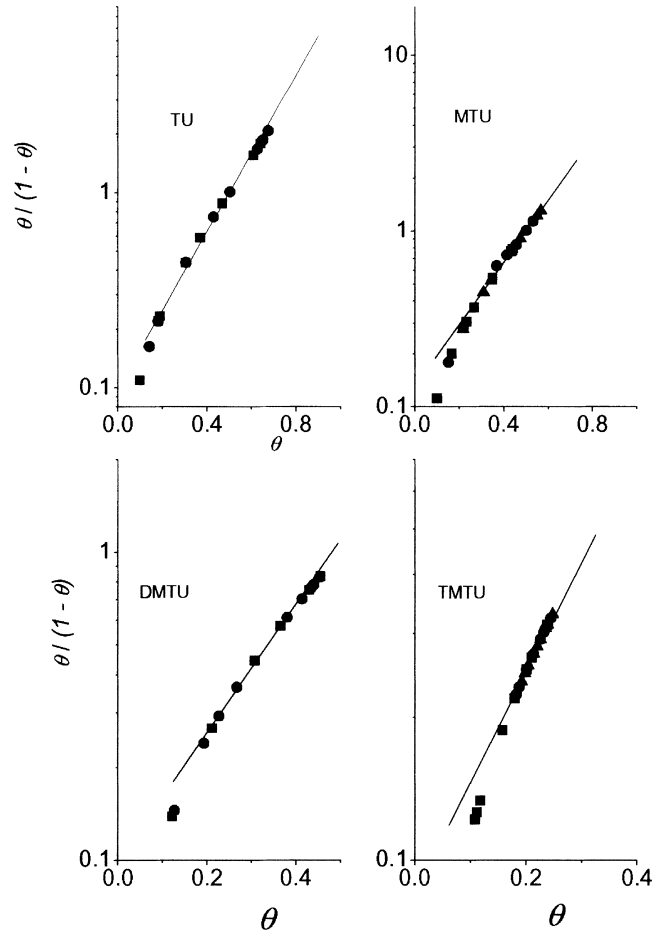


Fig. 8. $\theta_t/(1 - \theta_t)$ against θ_t plots for the adsorption of TU, MTU, DMTU and TMTU for different concentrations: (■) 0.01 mM; (▲) 0.1 mM; (●) 0.05 mM; $E_{ad} = 0.2$ V; 0.5 M H_2SO_4 ; 298 K.

at lower t_{ad} . According to previous works related to the adsorption of TU on Hg [22, 43], the adsorption processes can be described in terms of the empirical Frumkin isotherm for a homogeneous substrate where adsorbate–adsorbate interactions play a relevant role [44]. This behaviour is expected for an adsorption process where the adsorption energy depends linearly on the surface coverage by adsorbates [42]

$$\frac{\theta_t}{1 - \theta_t} = \frac{c_i}{55.5} \exp\left(-\frac{\Delta G_{ads}^\circ}{RT}\right) \exp(-a\theta_t) \quad (13)$$

Equation 13 involves ΔG_{ads}° , the standard Gibbs energy of adsorption of species i at zero coverage, c_i , the concentration of species i in solution, and a , the Frumkin interaction factor that is positive for attractive adsorbate–adsorbate interactions and negative for the repulsive interactions [45]. According to Equation 13 the θ values plotted as $\theta_t/1 - \theta_t$ against $\log \theta_t$ fulfil a linear relationship for the different TUs (Figure 8), and the value of a , within the experimental error, is practically the same, $a = -4.3 \pm 0.2$, indicating that repulsive adsorbate–adsorbate interactions are relevant. In principle, these interactions can be assigned either to

protonated neighbour –NH groups or, in the case of substituted thioureas, to the neighbour CH₃ groups. Repulsive interaction parameters close to 6 were reported for the adsorption of TU on mercury and gallium in aqueous sodium sulfate [44] and potassium nitrate [22] solutions and 16 for the case of TU adsorption on mild steel [17], whereas attractive interactions ($a = 1.4$) were reported for the case of TU adsorption on gold. Otherwise, from the extrapolation of the $\theta_t/1 - \theta_t$ against $\log \theta_t$ curves it results in $\Delta G_{\text{ads}}^\circ \approx 40 \pm 0.5$ kJ mol⁻¹ figure that can be compared to those found for the adsorption of TU on either gold [20] (43.3 kJ mol⁻¹) or mild steel [17] (42.95 kJ mol⁻¹) electrodes. It should be noted that in the present case, the standard state for the adsorption process is defined by the following equation [23]:

$$\frac{\theta_0}{1 - \theta_0} = \exp(-a\theta_0) \quad (14)$$

which for the case of $a = 4.3$ results in $\theta_0 \approx 0.25$.

5. Conclusions

1. TU and methyl TUs are strongly adsorbed on platinum under both open circuit and constant potential following an Elovich-type adsorption kinetics.
2. The degree of surface coverage by each adsorbate decreases according to the size of the molecule of TUs.
3. Adsorption data can be fitted to a Frumkin-type isotherm with $\Delta G_{\text{ads}}^\circ \approx 40 \pm 0.5$ kJ mol⁻¹ and a repulsive adsorbate–adsorbate interactions parameter $a = -4.3 \pm 0.2$.
4. The threshold potential for the electrooxidation of TU and methyl TUs is in the range 0.6 ± 0.05 V. A first electrooxidation stage, in the range of potentials from 0.4 to 0.9 V, involves the formation of –S–S–bond-containing products via partial deprotonation, the yield of the reaction decreasing with the number of methyl groups in the molecule.
5. A second electrooxidation stage takes place at $E > 0.9$ V leading to complete electrooxidation of products from the first electrooxidation stage. This electrooxidation stage can be described as a complex reaction under intermediate kinetics in the presence of adsorbed residues. The electrooxidation of adsorbates at this stage competes with the formation of the oxygen-containing monolayer.
6. Adsorbate intermediates decompose yielding sulfur residues which are electro-oxidized for $E > 0.9$ V.

Acknowledgements

This work was financially supported by the Consejo Nacional de Investigaciones Científicas y Técnicas

(CONICET), Agencia Nacional de Promoción Científica y Tecnológica of Argentina (PICT 98 06-03251) and the Comisión de Investigaciones Científicas de la Provincia de Buenos Aires (CIC).

References

1. D. Pletcher and F. Walsh, 'Industrial Electrochemistry' (Chapman & Hall, London, 1990).
2. D. Gabe, 'Principles of Metal Surface Treatment and Protection', (Pergamon, Oxford, 1978).
3. S. Mendez, G. Andreassen, P.L. Schilardi, M. Figueroa, L. Vázquez, R.C. Salvarezza and A.J. Arvia, *Langmuir* **14** (1998) 2515.
4. D.N. Upadhyay and V. Yegnaraman, *Mat. Chem. Phys.* **62** (2000) 247.
5. V.S. Martín, S. Sanlloriente and S. Palmiero, *Electrochim. Acta* **44** (1998) 579.
6. L. Müller, G.N. Mansurov and O.A. Petrii, *J. Electroanal. Chem.* **96** (1979) 159.
7. O.E. Piro, R.C.V. Piatti, A.E. Bolzán, R.C. Salvarezza and A.J. Arvia, *Acta Cryst.* **B56** (2000) 993.
8. A.E. Bolzán, I.B. Wakenge, R.C.V. Piatti, R.C. Salvarezza and A.J. Arvia, *J. Electroanal. Chem.* **501** (2001) 241.
9. A.E. Bolzán, I.B. Wakenge, R.C. Salvarezza and A.J. Arvia, *J. Electroanal. Chem.* **475** (1999) 181.
10. A.E. Bolzán, A.S.M.A. Haseeb, P.L. Schilardi, R.C.V. Piatti, R.C. Salvarezza and A.J. Arvia, *J. Electroanal. Chem.* **500** (2001) 533.
11. A.S.M.A. Haseeb, P.L. Schilardi, R.C.V. Piatti, A.E. Bolzán, R.C. Salvarezza and A.J. Arvia, *J. Electroanal. Chem.* **500** (2001) 543.
12. G. Horanyi, E.M. Rizmayer and P. Joó, *J. Electroanal. Chem.* **149** (1983) 221.
13. D. Papapanayiotou, R.N. Nuzzo and R.C. Alkire, *J. Electrochem. Soc.* **145** (1998) 3366.
14. G.M. Brown, G.A. Hope, D.P. Schweinsberg and P.M. Fredericks, *J. Electroanal. Chem.* **380** (1995) 161.
15. G.M. Brown and G.A. Hope, *J. Electroanal. Chem.* **413** (1996) 153.
16. A. Lukomska, S. Smolinski and J. Sobkowski, *Electrochim. Acta* **46** (2001) 3111.
17. B.G. Ateya, B.E. El-Anadouli and F.M. El-Nizamy, *Corros. Sci.* **24** (1984) 497.
18. Z.Q. Tian, W.H. Li, B.W. Mao and J.S. Gao, *J. Electroanal. Chem.* **379** (1994) 271.
19. J.O. Bockris, M.A. Habib and J.L. Carbajal, *J. Electrochem. Soc.* **131** (1984) 3032.
20. R. Holze and S. Shomaker, *Electrochim. Acta* **35** (1990) 613.
21. Z.Q. Tian, Y.Z. Lian and M. Fleischmann, *Electrochim. Acta* **35** (1990) 879.
22. R. Parsons and P. Symons, *Trans. Faraday Soc.* **64** (1968) 1077.
23. B.E. Conway, H. Angerstein-Kozłowska and H.P. Dhar, *Electrochim. Acta* **19** (1974) 455.
24. R. Woods, in A.J. Bard (Ed.), 'Electroanalytical Chemistry', Vol. 9 (Marcel Dekker, New York, 1976), ch. 1, p. 98.
25. E.E. Farndon, F.C. Walsh and S.A. Campbell, *J. App. Electrochem.* **25** (1995) 574.
26. D.R. Turner and G.R. Johnson, *J. Electrochem. Soc.* **109** (1962) 382.
27. E. Lamy-Pitara, L. Bencharif and J. Barbier, *Electrochim. Acta* **30** (1985) 971.
28. Y.E. Sung, W. Chrzanowski, A. Zolfaghari, J. Jerkiewicz and A. Wieckowski, *J. Am. Chem. Soc.* **119** (1997) 194.
29. S.I. Zhdanov, in A.J. Bard (Ed.), 'Encyclopedia of Electrochemistry of the Elements', Vol. IV (Marcel Dekker, New York, 1975), ch. 6.

30. M. Yan, K. Liu and Z. Jiang, *J. Electroanal. Chem.* **408** (1996) 225.
31. P. Schilardi, A.E. Bolzán, R.C.V. Piatti, C. Gutiérrez and A.J. Arvia, in preparation.
32. B. Beden, C. Lamy, N.R. de Tacconi and A.J. Arvia, *Electrochim. Acta* **35** (1990) 691.
33. V.P. Vasil'ev, V.I. Shorokhova, A.V. Katrovtseva and G.S. Lamakina, *Elektrokhimiya* **19** (1983) 453.
34. D.S. Tarbell, in N. Kharasch (Ed.), 'Organic Sulfur Compounds', Vol. 1 (Pergamon, New York, 1961), ch. X.
35. M. Fleischmann, I.R. Hill and G. Sundholm, *J. Electroanal. Chem.* **157** (1983) 359.
36. O. Azzaroni, B. Blum, R.C. Salvarezza and A.J. Arvia, *J. Phys. Chem B Lett.* **104** (2000) 1395.
37. V. Brunetti, B. Blum, P.L. Schilardi, R.C. Salvarezza and A.J. Arvia, *J. Phys. Chem.*, in press.
38. E.E. Reid, 'Organic Chemistry of Bivalent Sulfur', Vol. 5 (Chemical Publishing Co., New York, 1963).
39. M.W. Breiter, 'Electrochemical Processes in Fuel Cells', (Springer, Berlin, 1969).
40. A. Ulman, *Chem. Rev.* **96** (1996) 1533.
41. E. Bunge, R.J. Nichols, B. Roelfs, H. Meyer and H. Baumgärtel, *Langmuir* **12** (1996) 3060.
42. A.W. Adamson, 'Physical Chemistry of Surfaces' (John Wiley & Sons, New York, 1982).
43. A. Baars, J.W.J. Knapen, M. Sluyters-Rehbach and J.H. Sluyters, *J. Electroanal. Chem.* **368** (1994) 293.
44. G. Pezzatini, M.R. Moncelli and R. Guidelli, *J. Electroanal. Chem.* **301** (1991) 227.
45. A.J. Bard and L.R. Faulkner, 'Electrochemical Methods' (John Wiley & Sons, New York, 1980).